



Effects of various heat treatment cycles on mechanical properties and wear resistance of 65Mn carbon steel

Amir Abbas MOJAHEDI¹, Seyed Abdolkarim SAJJADI¹, and Fatemehsadat SAYYEDAN^{1,*}

¹ Department of Materials Science and Engineering, Faculty of Engineering, Ferdowsi University of Mashhad, Mashhad 9177948944, Iran

*Corresponding author e-mail: sayyed@um.ac.ir

Received date:

3 September 2025

Revised date:

20 October 2025

Accepted date:

20 February 2026

Keywords:

65Mn carbon steel;
Tensile strength;
Hardness;
Toughness;
Wear

Abstract

The aim of the present study is to investigate the effect of various heat treatment cycles on mechanical properties and wear resistance of 65Mn carbon steel. For this purpose, five different heat treatment cycles including normalizing, austenitizing, quenching, and tempering were performed at different austenitization temperatures and tempering times. Subsequently, effects of the parameters on tensile strength, toughness, hardness, and wear resistance of the heat-treated samples were investigated. X-ray diffraction (XRD) and scanning electron microscopy (SEM) equipped with energy dispersive X-ray spectroscopy (EDS) were employed to analyze microstructure of heat-treated samples. To study the wear resistance of the samples after heat treatment, pin-on-disk wear test was conducted. The results revealed that the optimal mechanical and wear properties, including a hardness of 723 HV, a tensile strength of 1062 MPa, a fracture toughness of $14.7 \text{ J}\cdot\text{cm}^{-2}$, and a weight loss of 0.001 g, were achieved after the heat treatment cycle of normalizing at 850°C for 30 min, austenitizing at 780°C for 30 min, oil quenching, and then tempering at 200°C for 60 min. These results were obtained due to the achievement of a two-phase martensite-ferrite microstructure with the minimum initial austenite grain size among different austenitization temperatures.

1. Introduction

Steel parts are exposed to contact and wear in many industries. The desired mechanical properties such as hardness, tensile strength, wear resistance, and toughness can be achieved with heat-treatable steels such as 65Mn carbon steel [1]. The effect of heat treatment on steels can also be seen in other steel grades [2,3]. 65Mn carbon steel, also known as spring steel, is a material with high tensile strength, hardness, wear resistance, and toughness, especially after heat treatment. It is a popular choice for making various types of springs, such as valve springs, clutch springs, and brake springs in automotive industry, ball bearings, cutting tools, tractor suspension systems, agricultural implements and hand tools, friction clutches and brakes of large engineering machinery such as loaders and cranes. The chemical composition of this steel contains 0.65 wt% carbon, 0.96 wt% manganese, and 0.21 wt% silicon, which is not far from being expected such properties of hardness and wear resistance due to its high content of manganese. Since manganese improves the hardenability and stabilizes the austenite phase during quenching, it indirectly enhances the hardness and wear resistance of this high-carbon steel by promoting a more complete martensitic transformation [4–6].

65Mn steel sheets are particularly popular because this steel can be easily formed and processed, and subjected to hot or cold rolling operations, depending on the specific application requirements [7]. Some other reasons for the wide use of this steel include good weldability, quenching-tempering heat treatment capability, good weld hardness and low tendency to decarbonize, good cutting and machinability

[8]. In addition to being used in the manufacture of spring products, 65Mn steel can also play a role as a tool working under cyclic stress, heavy load, and severe wear, such as cutting and rotary blades [9].

Dalai *et al.* [10] reported that medium manganese steels can be used in applications subject to wear, such as train tracks. Ge *et al.* [4] concluded that the weight loss due to wear in modified medium manganese austenitic steel (MMAS) is reduced by ~30% compared to martensitic steel indicating the higher wear resistance of MMAS compared to martensitic steel.

In order to achieve the desired properties in steels, it is necessary to create a microstructure through heat treatment that simultaneously has high hardness, strength, and toughness. The best microstructure with aforementioned properties is a two-phase structure consisting of martensite and ferrite [11]. Over the past two decades, many researchers have investigated the effect of heat treatment on improving the mechanical properties of 65Mn steel. For instance, Li *et al.* [1] investigated the effect of quenching-tempering heat treatment on the hardness and tensile strength of 65Mn steel and concluded that the optimal heat treatment cycle including austenitizing at 780°C followed by tempering at 200°C resulted in a hardness of 1.61 HVC and a tensile strength of 1197.9 MPa.

In the present study, in order to achieve appropriate mechanical properties of 65Mn steel, five different heat treatment cycles including normalizing, austenitizing, quenching, and tempering were designed and performed at different temperatures and times. The hardness, tensile strength, toughness, and wear resistance of the heat-treated samples were measured and compared. Finally, the optimal heat

treatment cycle including the optimal tempering time and the optimal austenitization temperature was introduced to achieve maximum hardness, tensile strength, toughness, and wear resistance.

2. Materials and methods

In order to obtain a uniform microstructure including fine pearlite, normalizing heat treatment was performed on 65Mn carbon steel samples with dimensions of 10 mm × 10 mm × 10 mm and chemical composition of 0.65 wt% carbon, 0.96 wt% manganese, 0.21 wt% silicon, 0.04 wt% chromium, 0.03 wt% nickel, and 0.021 wt% phosphorus. Austenitizing was performed in the temperature range of 780°C to 850°C for 30 min and immediately quenched in oil to obtain the martensite phase. In order to avoid brittleness and to obtain appropriate toughness, the samples were tempered at 200°C for 1 h and 6 h to determine the effect of tempering time on the microstructure and mechanical properties. Different heat treatment cycles performed on 65Mn steel are presented in Table 1.

Since the unique mechanical properties have a significant relationship with the grain size of the primary austenite, annealing was performed at the austenitization temperature to estimate the grain size and reveal the grain boundaries of the primary austenite. First, in order to homogenize the initial microstructure, normalizing was performed at 850°C for 30 min. Then, the samples were austenitized in an electrical furnace (Azar 2018, Iran) at 780°C, 800°C, and 830°C for 30 min and cooled down in the furnace to room temperature. The microstructure of the metallographic samples was studied to determine the grain size of the primary austenite using ImageJ software.

After heat treatment, the samples were prepared for microstructure observations. First, the samples were grinded with SiC sandpaper with Numbers of 60 to 2000 and then polished with aluminum oxide particles. The samples were rinsed with ethanol and etched in 2% Nital etchant solution for 10 s. The resulting microstructures were studied using a scanning electron microscope (SEM, MIRA3 TESCAN, Czech Republic).

Hardness testing was performed using a Vickers hardness apparatus (COOPA-VH1, Iran) with a load of 30 kg and a dwell time of 10 s. Hardness testing was performed at six different points on the sample surface and the results were reported as average ± standard deviation.

Microhardness test was performed using microindentation apparatus (Koop, MH3, Iran) with 10 N loading and 10 s dwell time. The microhardness values of six different points of the sample were measured and the results were reported as average ± standard deviation.

Uniaxial tensile testing was performed using a machine (Zwick-Z250, Germany) at a rate of 0.002 s⁻¹ on sample M5 (without tempering),

samples M1 and M4 (to investigate the effect of tempering time), and samples M2, M3, and M4 (to investigate the effect of austenitizing temperature). In each cycle, three samples were subjected to tensile testing and the results were reported as average ± standard deviation. The area under the stress-strain curve was calculated and reported as fracture toughness.

The samples were prepared in the form of disks with a diameter of 5 cm and a thickness of 4 mm and were subjected to a pin-on-disk wear test (TSN-WTC03) in accordance with ASTM G99 standard under load of 70 N, sliding distance of 500 m, and disk rotation speed of 500 rpm. The weight of the samples before and after the wear test was measured and recorded using a 4-decimal scale (DLS-100-6). The changes in the friction coefficient of the samples during the wear test were recorded. Also, the surface morphology of the samples was examined using a scanning electron microscope (SEM, MIRA3 TESCAN, Czech Republic) to study the wear track followed by detection of the wear mechanism.

3. Results and discussion

3.1 Microstructure

The SEM images of the microstructure of samples M2, M3, and M4 after heat treatment cycles, as presented in Table 1, are shown in Figure 1. The martensitic phase is observed in the microstructure of 65Mn steel after heat treatment cycles. Li *et al.* [1] obtained the same result in a similar study on 65Mn steel. This outcome was not far from expectations, because by austenitizing and quenching 65Mn steel, there was no ability to form a phase other than the martensite phase. As can be seen in the microstructure image of all samples in Figure 1, there are veins in the structure that are contributed to the martensite phase. With more precision, it is possible to find out the vacancies of some phases. To find out the chemical composition of the phases, EDS analysis was performed. The results are presented in Figure 2. The analysis indicates the presence of iron and manganese elements in the phases. The EDS results were not enough to completely define the characteristics of the phases therefore, Vickers microhardness test was taken from these veins and the sample matrix. The Vickers microhardness test results showed that the average hardness of the martensitic matrix and the veins in sample M2 were 725 and 976 Vickers, respectively. These data revealed that this phase had much greater hardness than the martensitic matrix. Since 65Mn steel is a high-carbon steel containing manganese, and considering the heat treatment conditions that promote carbide precipitation, together with the very high microhardness values (~976 HV) and the morphology of the bright vein-like features, it is highly likely that these regions

Table 1. Various heat treatment cycles applied on 65Mn carbon steel.

Cycle sample	Normalizing		Austenitizing		Quenching medium	Tempering	
	Temperature [°C]	Time [min]	Temperature [°C]	Time (min)		Temperature [°C]	Time [h]
M1	850	30	830	30	Oil	200	6
M2	850	30	780	30	Oil	200	1
M3	850	30	800	30	Oil	200	1
M4	850	30	830	30	Oil	200	1
M5	850	30	830	30	Oil	-	-

correspond to cementite and manganese carbides. Although EDS could not directly detect carbon due to its limited sensitivity to light elements, the combined evidence from microhardness, morphology, and thermal history supports this interpretation.

In addition, although the microstructure is reported as dual-phase, it should be noted that the dominant phase in all heat-treated samples was martensite due to the high carbon content of 65Mn steel and oil-quenching treatment. A very small amount of ferrite/carbide regions was observed mainly along prior-austenite grain boundaries. The qualitative microstructural examination showed that the volume fraction of these secondary phases slightly decreased with increasing austenitizing temperature, as higher temperatures promoted further carbide dissolution prior to quenching. Since the fraction of ferrite/carbide was very small and did not significantly influence the main martensitic matrix behavior, quantitative phase fraction analysis was not included. This observation is also consistent with previously reported behavior of high-carbon Mn-alloyed steels subjected to quench-and-temper cycles.

Microstructure of steels is highly dependent on the history of the performed heat treatment cycles [12,13]. The presence of these veins is also related to the type of heat treatment that has been performed on the steel. As mentioned, the samples were normalized at the same temperature and time, but their austenite temperature and tempering time were different. Austenitizing begins from the critical temperature AC1. The critical temperature of 65Mn steel according to the report of Lee *et al.* [1] is approximately 730°C. Therefore, the structure consisting of pearlite and carbides slowly transforms into austenite with increasing temperature over 730°C. Moreover, with increasing temperature, the carbides begin to transform from a veined state to smaller spheres and then they are dissolved and instead, a solid solution

region is formed. At high austenitizing temperatures, as expected, less carbides are presented. As a result, hard phase martensite can be created by performing austenitizing, quenching, and tempering heat treatment and its properties against tensile and abrasion conditions can be utilized [14]. It should be mentioned that in sample M2, with the lowest austenitizing temperature among the heat treatment cycles, more veins of cementite can be observed.

3.2 Hardness

Hardness is an important parameter in the selection of parts for industrial applications. Since, 65Mn steel has a martensitic matrix, it is expected to exhibit high hardness. In this section, the factors and parameters affecting hardness will be reviewed.

According to the hardness test results shown in Figure 3, the highest hardness value was related to the sample M5, the sample without tempering heat treatment. It has been reported that industrial parts with martensitic structure should be tempered one or two times before entering the industry [15]. It is noteworthy that sample M5 was chosen solely to show the effect of tempering on microstructure, hardness, mechanical properties, and wear resistance. Sample M2 has the highest hardness among the other tempered specimens. This result is also in consistent with the observations of Li *et al.* [16]. Here, the aim is to investigate the effect of tempering heat treatment on the hardness of steels. To find out the reasons for the higher hardness of M2 sample, attention was paid to the parameters affecting the hardness of samples containing martensitic phase. The factors affecting the hardness of steels are the carbon content, age hardening, and the grain size. Among them, the grain size is one of the factors affecting the progress and growth of martensitic laths [15].

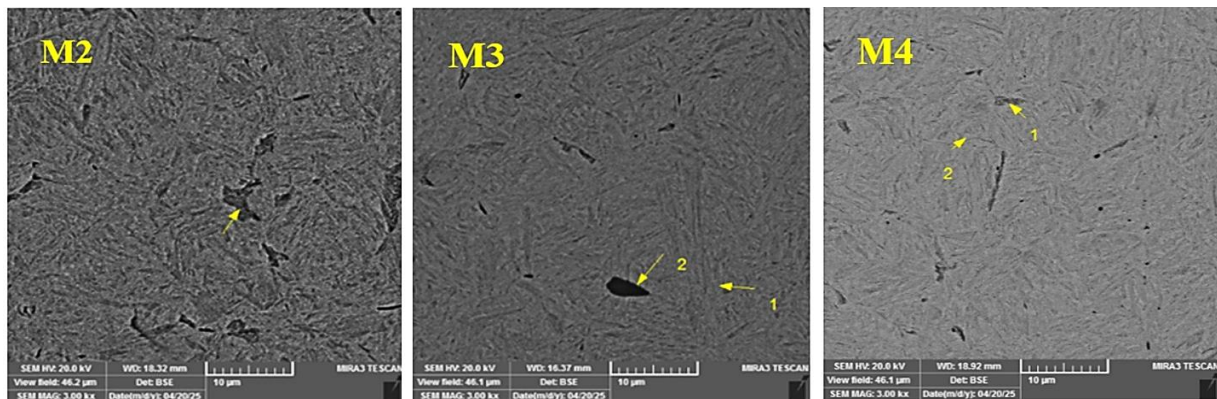


Figure 1. SEM images of the microstructure of samples M2, M3, and M4 after heat treatment cycles listed in Table 1.

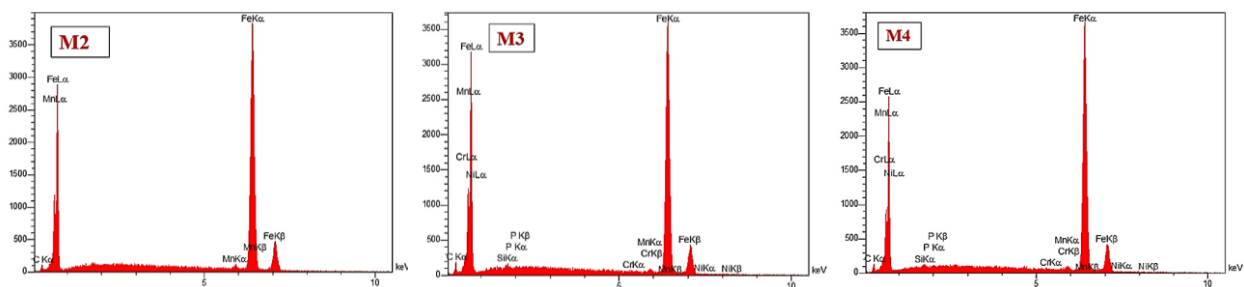
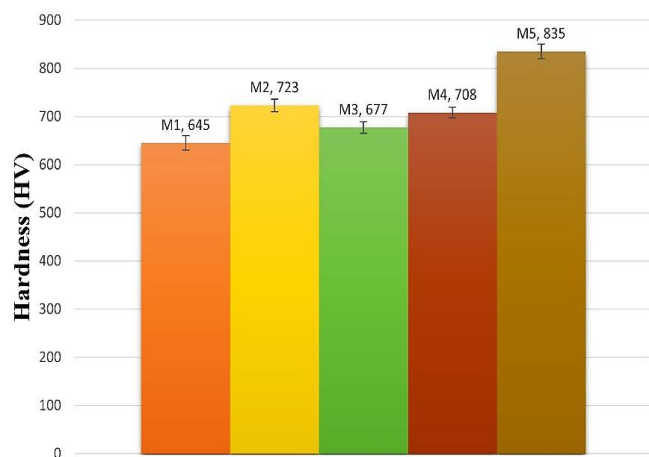


Figure 2. EDS analysis of the points marked in the SEM images presented in Figure 1 (the marked point of sample M2, point 2 of sample M3, and point 1 of sample M4).

Table 2. Uniaxial tensile test results.

Samples	Yield stress [MPa]	Ultimate tensile stress [MPa]	Fracture stress [MPa]	Fracture toughness [$\text{J}\cdot\text{cm}^{-2}$]	Ductility [Elongation %]
M1	765	1089	800	15000	15.5
M2	746	1058	749	14700	15.6
M3	772	1107	821	15500	15.8
M4	780	1102	825	14000	14.2
M5	778	1078	811	13000	13.3

**Figure 3.** Vickers hardness test results performed on different samples.

Although sample M3 exhibited a relatively fine austenite grain size and the presence of a noticeable number of undissolved carbides, its hardness was slightly lower than that of sample M4. This behavior can be explained by the combined influence of the austenitizing temperature on carbide dissolution and carbon distribution. At the austenitizing temperature of 800°C (sample M3), some carbides were partially dissolved, which reduced the carbon concentration in the austenite before quenching and consequently decreased the carbon supersaturation in the resulting martensite. In contrast, at 830°C (sample M4), a larger portion of carbides was dissolved into austenite, providing a higher amount of carbon available for martensitic transformation and resulting in a slightly higher hardness. Furthermore, the carbides in M3 were observed mainly at the grain boundaries rather than being uniformly dispersed in the matrix, which limited their strengthening contribution. Therefore, the hardness difference between M3 and M4 is attributed not only to grain size but also to the extent of carbide dissolution and carbon partitioning during austenitization.

According to Wang *et al.* [11], one of the factors affecting the hardness of the 65Mn steel samples is the grain size of the primary austenite. Considering the dependence of the grain size on the temperature and time of austenitization and in order to obtain the grain size, the samples were initially normalized and then austenitized at the same temperature and cooled in air. The grain size was measured using ImageJ software after metallographic preparations. It was found that the sample austenitized at 780°C with the grain size of $4.5\pm 1.4\ \mu\text{m}$ had the smallest grain size of primary austenite. Coarser grains were obtained with primary austenite grain sizes of $5.7\pm 2.4\ \mu\text{m}$ and $7.3\pm 2.1\ \mu\text{m}$ at austenitizing temperatures of 800°C and 830°C, respectively.

As mentioned in part 3.1, some carbides were observed in the microstructure of sample M2. These carbide were appeared more in

sample M2 than other ones which are one of the factors causing fine primary austenite grains. These carbides prevent grain growth by pinning and locking of primary austenite grain boundaries. The pinning effect has also been reported by other researchers [18-20]. Because the austenitization temperatures of 780°C and 800°C are not sufficient to dissolve carbides and form a solid solution, these carbides are present and cause the pinning effect. Moreover, the effect of the austenitization temperature on grain growth cannot be ignored. A finer grain size was obtained at austenitization temperature of 780°C compared to other samples austenitized at higher temperatures. The effect of this factor can be observed clearly in parts 3.3 and 3.4 in achievement of superior mechanical properties and wear resistance for the sample M2. These effects lead to the creation of many grain boundaries and, as a result, greater resistance to deformation and hardness. The finer the grain size of the initial austenite, the higher the density of martensite plates per unit volume and therefore the hardness of martensite increases [15]. In addition to the fine grain size in sample M2, the presence of a larger amount of cementite and undissolved carbide in this sample also caused greater hardness. However, the hardness value of 65Mn steel is related to the martensitic phase, the impact of carbides cannot be ignored [21].

By carefully examining other samples, in addition to the effect of austenitization temperature and primary austenite grain size on hardness, the effect of tempering time on the hardness value can be observed. Islami *et al.* [17] reported that the hardness of martensitic steel decreases after tempering, but the toughness and flexibility increase. This result can be clearly seen in the comparison of samples M4 and M5. Also, by more carefully examining sample M1, the effect of tempering time can be observed in the results obtained, such that the hardness decreases with a longer tempering time.

3.3 Tensile strength

Table 2 presents the mechanical properties including fracture stress, fracture toughness, ultimate tensile stress (UTS), ductility (elongation), and yield strength. Accordingly, the heat treatment cycles of sample M3 has the best mechanical properties including tensile strength and fracture toughness. The results obtained from the hardness test and the investigation of the microstructure and heat treatment steps performed on the samples were referred to find out the reason. Sample M1 revealed desired properties after sample M3. It has been reported that toughness decreases with increasing hardness [33]. Although sample M2 has weaker mechanical properties than M3, sample M2, despite having the highest hardness, exhibits very good mechanical properties that cannot be ignored. Furthermore, these properties are better displayed in abrasion resistance. The hardness test results show that samples M2 and M3 have the highest hardness

value among the tempered samples, and sample M2 has a higher hardness than sample M3. Since sample M2 has a finer primary austenite grain size than M3, it should have greater toughness based on the principles of materials science. On the other hand, sample M2 has a larger volume of carbides, which causes it to have lower toughness than M3. M5 sample was not subjected to tempering heat treatment and therefore has high hardness and brittleness. According to Islami *et al.* [17], tempering heat treatment on martensitic steels within a certain temperature range causes the brittleness, internal stresses and dislocations to avoid the transformation into martensitic phase with higher toughness. It should be mentioned that martensitic steels are tempered once or even more times before entering the industry [15].

The effect of austenitization temperature can be observed in the yield stress. It is worth noting that as the austenitization temperature increases, the yield stress increases because more austenite is produced, which is later converted into more martensite by quenching [22]. In addition to the austenitization temperature, tempering heat treatment also increases the yield stress due to the rearrangement of the microstructure and grains [23]. These results were also observed in sample M4, which obtained the highest yield stress with the austenitization temperature of 830°C (the highest austenitization temperature among the samples) and tempering.

By comparing samples M1 and M4, it can be seen that there was not much difference in the tensile test results with the same normalizing, austenitizing, and quenching conditions. Only the tempering time caused an evident difference. Comparing the tensile test results of samples M1 and M4, the effect of tempering time on the mechanical properties of steels, especially in 65Mn carbon steel, can be recognized. However, sample M1 had higher flexibility and toughness than sample M4 due to the longer tempering time, and sample M4 had the optimal yield, tensile, and fracture stresses.

Although the grain refinement and the presence of hard carbide phases generally enhance the yield strength of steels, sample M2 exhibited a lower yield strength than M4 despite having the smallest austenite grain size and the highest number of hard phases. This behavior can be explained by the combined effects of austenitizing temperature and carbon distribution. At the lower austenitizing temperature of 780°C (sample M2), some carbides remained undissolved, resulting in a non-uniform carbon distribution and lower carbon concentration in the austenite prior to quenching. Consequently, the martensitic matrix of M2 contained less supersaturated carbon and a larger number of interfaces between martensite and undissolved carbides, which acted as local stress-relief sites and reduced the effective yield strength. In contrast, the higher austenitizing temperature of 830°C in sample M4 promoted more complete dissolution of carbides and a more homogeneous carbon enrichment of the austenite, which led to the formation of a stronger and more uniform martensitic structure upon quenching. Therefore, despite the coarser grain size, sample M4 exhibited a higher yield strength than M2.

3.4 Wear test

In the present study, pin-on-disk wear test was performed on five 65Mn steel samples and their results were presented as weight loss. Figure 4 shows the weight loss in the wear test accompanied with the

hardness values of the samples. By observing the graph, it is clear that sample M1 has the lowest hardness and the highest weight loss among the specimens. It is observed that samples M2 and M3 with lower hardness, show better wear resistance than the as-quenched sample (M5). As a result, wear resistance is not always directly related to hardness. The same result was also presented by Jha [24] and Rendon *et al.* [25]. They reported that increasing hardness initially leads to lower wear rate due to the resistance of the sample surface to the destructive action of abrasive particles. With further increase in hardness beyond a critical value, the wear rate increases because of the brittle fracture of the material due to the presence of hard phases [22].

With more precision, Figure 4 shows that sample M2 has the lowest weight loss and the best performance against abrasion among other samples. It is worth mentioning that sample M2 has the highest hardness among the tempered samples, so it can be concluded that with the hardness of sample M2 (723 HV) the relationship between abrasion resistance and hardness is direct. However, comparing the abrasion resistance of sample M2 with sample M5 shows that sample M5, having a higher hardness (835 HV) than sample M2, has lower abrasion resistance. This hardness is in the same range where abrasion resistance and hardness are inversely related.

Xu *et al.* [26] reported that in addition to hardness, grain refinement is also an effective way to increase yield strength without decreasing ductility. Therefore, grain refinement can be expected as an effective solution to improve wear resistance. This result has also been reported by other researchers [27-31]. By measuring the grain size of the primary austenite, it is determined that the smallest grain size of the primary austenite is related to the heat treatment cycle of the sample M2, which has the best wear resistance. As mentioned, the reason for this phenomenon is the pinning of grain boundaries of the primary austenite by carbides (pinning effect).

It can also be seen that in samples M2 and M3 with the lowest weight loss, another reason can be obtained with more accuracy in the microstructure of the samples. Veins of cementite can be observed in the microstructure of these samples with high hardness and brittleness. These hard cementite veins cause to achieve appropriate wear resistance. This result has also been reported by Chenje *et al.* [32].

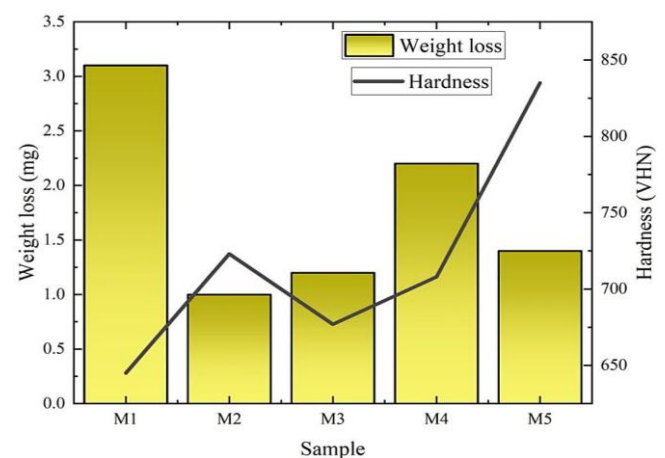


Figure 4. Pin-on-disk wear test results presented based on weight loss along with hardness test results.

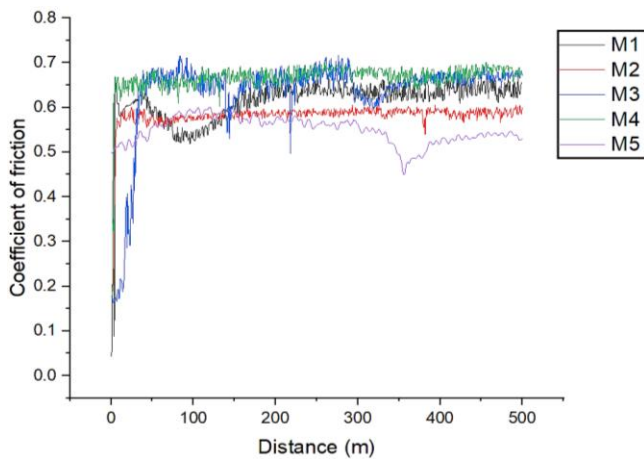


Figure 5. Friction coefficient results of the pin-on-disk wear test.

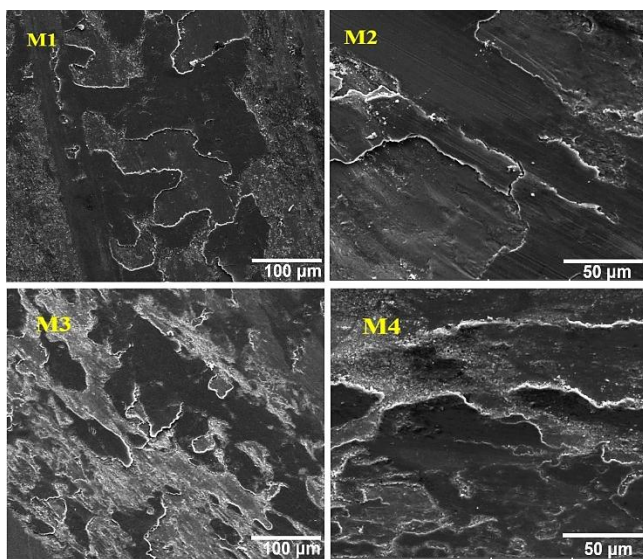


Figure 6. SEM images of the tracks formed during wear test on different samples.

Considering the friction coefficient versus sliding distance graph for samples M1 to M5 in Figure 5, it can be clearly seen that sample M2 has the lowest friction coefficient with the smallest range of variation among the quenched-tempered samples. This favorable frictional behavior is attributed to the two-phase structure of ferrite-martensite and carbide and a combination of hardness and toughness.

According to the SEM images of the wear track presented in Figure 6, it is clear that the delamination wear mechanism has been occurred. In this mechanism, the laminar surfaces appear congregated with shallow depth due to the non-uniform release of stress. There are two theories to explain the delamination wear mechanism. The first theory presented by Shu [34] states that dislocations accumulate below the surface as the slip distance increases, and thus, the dislocation density increases. The dislocations connect together and form cavities. The cavities connect over time, forming cracks along the surface. Eventually, when a crack reaches a critical length, the material between the crack and the surface separates from the surface as a sheet.

The second theory conducted by Jahanmir *et al.* [35] involves “surface tension or compressive stress accumulation”. According to this theory, when two sliding surfaces come into contact, the surface

ridges of the softer surface deform and break due to cyclic loading. The surface ridges of the harder surface shear the softer surface, resulting in surface tension.

It should be noted that the delaminated flakes observed in Figure 6 do not represent individual carbides but wear fragments produced by subsurface crack growth and linking during sliding. These flakes may contain carbides embedded in martensitic plates, therefore their size does not directly correspond to the carbide morphology observed in Figure 1. The presence of undissolved carbides promoted crack initiation at grain and lath boundaries; however, the final flake dimensions are governed by the delamination mechanism.

Enayati *et al.* [34] reported that cracks start to nucleate below the surface and gradually propagate along the surface. The depth of crack propagation depends on the material properties and the friction coefficient. The cracks cut through the surface layers at weak areas and create planar wear debris. The thickness of the planar particles depends on the position of crack growth below the surface, which is controlled by the vertical and tangential forces.

Comparing the wear test results and SEM images of the heat-treated samples, a good agreement between the results is observed. The flakes that have separated from the surface during the delamination wear mechanism are in fact the same carbides observed in the SEM images presented in Figure 1.

By comparing the results of hardness, tensile, and wear tests, it can be concluded that sample M2, with the highest hardness and the lowest weight loss in the wear test and with a tiny deviation from sample M3 in the tensile test, is the best heat treatment cycle design for 65Mn steel. With such a heat treatment design, the best mechanical properties with desired wear resistance can be obtained for 65Mn steel.

4. Conclusions

- 1) The most optimized heat treatment cycle for 65Mn steel, which can be achieved by the highest hardness, tensile stress, fracture toughness, and wear resistance, is normalizing at 850°C, austenitizing at 780°C, oil quenching, and tempering at 200°C for 60 min.
- 2) Although the microstructure consisted of a martensitic matrix with a minor fraction of ferrite/carbide, the martensite phase was dominant in all conditions. The amount of ferrite/carbide showed only slight qualitative reduction with increasing austenitizing temperature due to enhanced carbide dissolution prior to quenching. However, this minor phase fraction did not alter the overall trend in mechanical and wear properties, which were mainly governed by martensite morphology and grain refinement.
- 3) Wear resistance in steels is not always directly related to the hardness of steel.
- 4) Wear resistance is associated with grain size and toughness of steels, and the most optimized wear resistance occurs when steel is optimized in terms of hardness, toughness, grain size, and generally mechanical properties.
- 5) The wear mechanism of 65Mn steel was delamination wear in which thin sheets of cementite and manganese carbides were detached from the surface.

6) By performing proper heat treatment and regarding the pinning effect, desired grain size can be achieved, which will result in excellent mechanical and wear properties.

Conflict of interests

The authors have declared no conflict of interest.

Acknowledgments

The authors acknowledge support of Ferdowsi University of Mashhad on this research.

References

- [1] A. Li, M. Hu, and X. Wang, "Influence of sub-temperature quenching temperature on microstructure and property of 65Mn steel," *Advanced Materials Research*, vol. 102–104, pp. 460–464, 2010.
- [2] P. Apichai, "Influence of six-step heat treatment on microstructures and mechanical properties of 5160 alloy steel," *Journal of metals, Materials and minerals*, vol. 32, no. 1, pp. 72–78, 2022.
- [3] P. Apichai, "Effects of quenchants on microstructures and mechanical properties of steel grade AISI 5160," *Journal of metals, Materials and minerals*, vol. 30, no. 3, pp. 15–23, 2020.
- [4] S. Ge, Q. Wang, and J. Wang, "The impact wear-resistance enhancement of medium manganese steel and its application in mining machines," *Wear*, vol. 376, no. 377, pp. 1097–1104, 2017.
- [5] G. Huang, G. Jiao, D. Wen, Ch. Zhou, and K. Wu, "Mechanical properties of heat treated 65Mn steel produced by compact strip production," *Advanced materials research*, vol. 168, no. 170, pp. 832–836, 2011.
- [6] M. A. Hafeez, "Microstructural and mechanical properties of one-step quenched and partitioned 65Mn steel," *Arabian Journal for Science and Engineering*, vol. 46, pp. 2261–2267, 2021.
- [7] S. N. Ghali, and M. K. El-Fawkhry, "Simulation of cooling process effect on mechanical properties of 65Mn strip," *Materials Science, Engineering*, 2015.
- [8] Y. Huang, and G. Zhang, "Microstructure and property of 65Mn steel preheated by laser strengthening," *Transactions of the Chinese Society of Agricultural Engineering*, vol. 31, no. 1, pp. 53–57, 2015.
- [9] A. Li, and M. Hu, "Microstructure and properties of 65Mn steel after austenite inverse phase transformation by sub-temperature quenching," *Advanced materials research*, vol. 194, no. 196, pp. 89–94, 2011.
- [10] R. Dalai, S. Das, and K. Das, "Effect of thermos-mechanical processing on the low impact abrasion and low stress sliding wear resistance of austenitic high manganese steels," *Wear*, vol. 420, no. 421, pp. 176–183, 2019.
- [11] Y. Wang, J. Sun, T. Jiang, C. Yang, Q. Tan, S. Guo, and Y. Liu, "Super strength of 65Mn spring steel obtained by appropriate quenching and tempering in an ultrafine grain condition," *Materials Science and Engineering: A*, vol. 754, pp. 1–8, 2019.
- [12] B. C. Kandpal, D. K. Gupta, A. Kumar, A. K. Jaisal, A. K. Ranjan, A. Srivastava, and P. Chaudhary, "Effect of heat treatment on properties and microstructure of steels" *Materials Today: Proceedings*, vol. 44, pp. 199–205, 2021.
- [13] M. S. Htun, S. T. Kyaw, and K. T. Lwin, "Effect of heat treatment on microstructures and mechanical properties of spring steel," *Materials and Minerals*, vol. 18, no. 2, pp. 191–197, 2008.
- [14] L. D. Barlow, and M. D. Toit, "Effect of austenitizing heat treatment on the microstructure and hardness of martensitic stainless steel AISI 420," *Journal of materials engineering and performance*, vol. 21 pp. 1327–1336, 2012.
- [15] M. A. Golozar, *Fundamental and application of heat treatment of steels and cast irons*, (Ed) IUT Publication, 7th Print 2008.
- [16] A. Li, "Influence of pretreatment process on microstructure and properties of 65Mn steel after subcritical quenching," *Mechanics and Materials*, vol. 310, pp. 55–58, 2013.
- [17] N. M. Islami, N. A. Amir Khatif, M. Kecik, and M. Shaharudin, "The effect of heat treatment on the hardness and impact properties of medium carbon steel," *Materials Science and Engineering*, vol. 144, p. 012108, 2016.
- [18] K. Song, and M. Aindow, "Grain growth and particle pinning in a model Ni-based superalloy," *Materials Science and Engineering*, vol. A 479, pp. 365–372, 2008.
- [19] M. Apel, B. Bottger, J. Rudnizki, Ph. Schaffnit, and I. Steinbach, "Grain growth simulations including particle pinning using the multiphase-field concept," *ISIJ International*, Vol. 49, no. 7, pp. 1024–1029, 2009.
- [20] T. Zhou, H. Zurob, R. Omalley, and K. Rehman, "Model Fe-Al steel with exceptional resistance to high temperature coarsening Part I: Coarsening mechanism and particle pinning effects," *Metallurgical and Materials Transactions A*, vol. 46, no. 1, pp. 178–189, 2015.
- [21] W. Liu, X. Wang, F. Guo, and Ch. Shang, "Carbides dissolution in 5Cr₁₅MoV martensitic stainless steel and new insights into its effect on microstructure and hardness," *Materials*, vol. 15, p. 8742, 2022.
- [22] C. A. Suski, and C. A. S. Oliveira, "Effect of austenitization temperature on the precipitation of carbides in quenched low carbon boron steel," *Metallography, Microstructure, and Analysis*, vol. 2, pp. 79–87, 2013.
- [23] T. Senthilkumar, and T.K. Ajiboye, "Effect of heat treatment processes on the mechanical properties of medium carbon steel," *Journal of Minerals & Materials Characterization & Engineering*, vol. 11, no. 2, pp. 143–152, 2012.
- [24] A. Jha, B. K. Prasad, O. P. Modi, and S. Das, A. H. Yegneswaran, "Correlating microstructural features and mechanical properties abrasion resistance of a high strength low alloy steel," *Wear*, vol. 254, pp. 120–128, 2003.
- [25] J. Rendon, and M. Olsson, "Abrasive wear resistance of some commercial abrasion resistant steels evaluated by laboratory test methods," *Wear*, vol. 267, pp. 2055–2061, 2009.

- [26] X. Xu, W. Xu, F. H. Ederveen, and S. Zwaag, "Design of low hardness abrasion resistant steels," *Wear*, vol. 310, pp. 89–93, 2013.
- [27] G. Bregliozzi, A. Di Schino, J. M. Kenny, and H. Haefke, "The influence of atmospheric humidity and grain size on the friction and wear of AISI 304 austenitic stainless steel," *Materials Letters*, vol. 57, pp. 4505–4508, 2003.
- [28] D. Bhattacharyya, A. Hajra, A. Basu, and S. Jana, "The effect of grain size on the wear characteristics of high-speed steel tools," *Wear*, vol. 42, pp. 63–69, 1977.
- [29] S. Gündüz, R. Kaçar, and H. Ş. Soykan, "Wear behavior of forging steels with different microstructure during dry sliding," *Tribology International*, vol. 41, no. 5, pp. 348–355, 2008.
- [30] L. Zhou, G. Liu, Z. Han, and K. Lu, "Grain size effect on wear resistance of a nanostructured AISI52100 steel," *Scripta Materialia*, vol. 58, pp. 445–448, 2008.
- [31] A. Sundstrom, J. Rendon, and M. Olsson, "Wear behavior of some low alloyed steels under combined impact/abrasion contact conditions," *Wear*, vol. 250, pp. 744–754, 2001.
- [32] T. W. Chenje, D. J. Simbi, and E. Navara, "Relationship between microstructure, hardness, impact toughness and wear performance of selected grinding media for mineral ore milling operations," *Materials and Design*, vol. 25, pp. 11–18, 2004.
- [33] S. A. Sajjadi, "Mechanical Behavior of Materials (Ed)," Ferdowsi University of Mashhad Publication, 7th Print, 2022.
- [34] K. Enayati, and F. Sayyedani, "Study of dry sliding wear behavior of Ti-48Al-2Nb-2Cr alloy," *Tribology - Materials, Surfaces & Interfaces*, vol. 16, no. 2, p. 1881876, 2022.
- [35] S. Jahanmir, N. P. Suh, and E. P. Abrahamson II, "The delamination theory of wear and the wear of a composite surface," *Wear*, vol. 32, no. 1, pp. 33–49, 1975.